Atomic Force Microscope and Surface Plasmon Resonance Investigation of Polymer Blends of Poly([2-(methacryloyloxy)ethyl]phosphorylcholine-*co*-lauryl methacrylate) and Poly(lauryl methacrylate)

Stuart Clarke, Martyn C. Davies, Clive J. Roberts,* Saul J. B. Tendler, and Philip M. Williams

Laboratory of Biophysics and Surface Analysis, School of Pharmaceutical Sciences, The University of Nottingham, Nottingham NG7 2RD, U.K.

Andrew L. Lewis and Vincent O'Byrne

Biocompatibles Ltd., Farnham Business Park, Weydon Lane, Farnham, GU9 8QL U.K.

Received September 26, 2000; Revised Manuscript Received March 5, 2001

ABSTRACT: To rationally design new synthetic polymers for use in vivo, it is necessary to characterize the surface of the material to understand the interactions that occur when exposed to biological environments. Incorporation of phosphorylcholine (PC) into polymers has been shown to improve biocompatibility by suppressing unfavorable responses which occur on contact with body fluids. Here, polymer blends of [2-(methacryloyloxy)ethyl]phosphorylcholine-*co*-lauryl methacrylate (MPC-*co*-LMA (1:6 mole ratio)) and poly(lauryl methacrylate) (PLMA) have been produced with varying ratios of the two components. The surface of the blends when coated onto silver has been characterized using tapping mode atomic force microscopy (TMAFM) and surface plasmon resonance (SPR). Analysis has revealed that the blends formed by the two polymers are immiscible and exhibit surface segregation with nanometer-sized domains being formed throughout the range of the mixtures. The MPC-*co*-LMA is preferentially expressed at the surface of the blends leading to enhanced protein-resistant properties.

Introduction

The field of biomaterials has seen a massive increase in investment and research over the past 20 years in the hope of finding materials that can be put in direct contact with living systems with no adverse effects. A large number of materials are currently in routine use in the medical industry including metals, ceramics, and polymers, and although they have excellent physical and mechanical properties, none are ideal for prolonged use in vivo due to their lack of biocompatibility.[1] When placed in biological fluids such as blood or urine, the material is identified by the host as being foreign, resulting in unfavorable responses. In the case of blood, protein adsorption and platelet adhesion initiate the activation of the clotting cascade which results in the production of a potentially fatal thrombus. This can be particularly problematic in procedures involving blood contact with the large surface area of a medical device, for example, a cardiopulmonary bypass operation. Administration of heparin is commonly used to counter this effect, but this can lead to uncontrolled bleeding.[2] Less serious problems occur with other bodily fluids: Urinary catheters can be blocked as a result of mineral encrustation while contact lenses suffer from protein deposition, both conditions leading to unnecessary discomfort to the wearer.

Synthetic polymers appear to offer a potential solution due to the ability to tailor their mechanical and surface chemical properties to suit the environment in which they are used. Phosphorylcholine (PC) is the major headgroup found in the phospholipids which make up the extracellular matrix of red blood cells, and PC-containing materials have been shown to exhibit excellent biocompatibility,[3] reducing protein adsorption,[4,5] platelet adhesion,[6] and thrombus formation,[7] therefore eliminating many of the problems associated with surface fouling. By mimicking the phospholipid bilayer found on the outer surface of cells, these materials effectively disguise themselves as a natural component of the environment in which they are placed, and many examples of different polymeric materials that employ PC to enhance protein resistance have been produced.[8−13]

As an alternative to synthesizing new PC-containing polymers, polymer blends offer the opportunity to further investigate the surface properties of PC in new materials. By blending two or more polymers together, materials may be produced with characteristics of the constituents but having overall properties different than any of the single components. A common occurrence in such polymer blends is that of phase segregation.[14−16] If the components of the blend are not fully miscible, then the resulting mixture can contain defined regions of each of the original polymers. When phase segregation is identified in a blend, it is often accompanied by preferential expression of one of the components at the surface. Since it is the surface which is of most importance in defining the in-vivo performance of a material, it is important to characterize the surface as well as the bulk properties.

Over the past decade atomic force microscopy (AFM) has emerged as a powerful technique for imaging the surface of materials, and when used in tapping mode (TMAFM), it may distinguish between the components of a polymer blend which have different viscoelastic

* To whom correspondence should be addressed. Telephone +44 (0) 115 9515048; Fax +44 (0) 115 9515110; E-mail Clive.Roberts@Nottingham.ac.uk.

10.1021/ma0016681 CCC: $20.00
Published on Web 05/11/2001

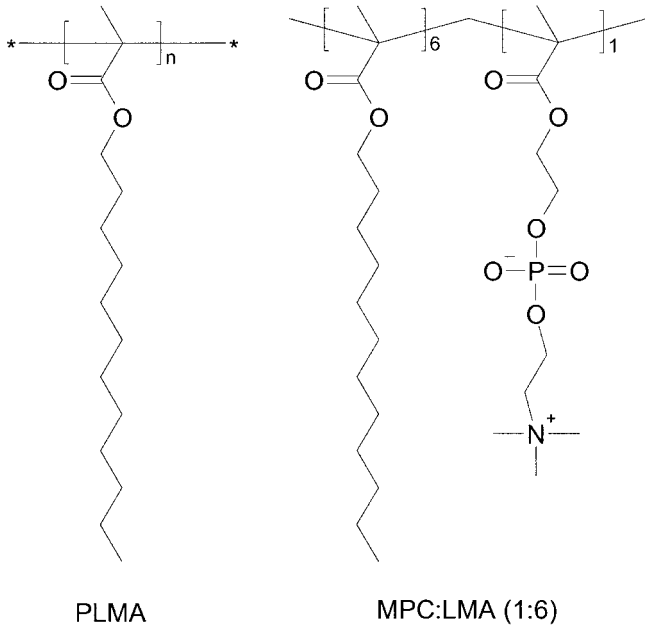

Figure 1. Chemical structures of the two blend components: poly(lauryl methacrylate) (PLMA) and the copolymer [2-(methacryloyloxy)ethyl]phosphorylcholine-*co*-lauryl methacrylate (1:6) (MPC-*co*-LMA).

properties.[17,18] Surface plasmon resonance (SPR) is an analytical technique that can probe surface interactions in real time and has been used to study a variety of surface events including erosion of biodegradable polymer blends[19] and interactions of proteins with surfaces.[20,21] Nakabayashi and co-workers have previously investigated the use of PC polymers as additives to segmented polyurethanes and reported the resulting enhanced biocompatibility.[22,23] They also noted that the PC polymer becomes concentrated in the surface region of the material when membranes are formed from the materials.[24] Here, we employ AFM and SPR to investigate the topography and biocompatibility of blends of poly([2-(methacryloyloxy)ethyl]phosphorylcholine-*co*-lauryl methacrylate) in a 1:6 mole ratio (MPC-*co*-LMA) and poly(lauryl methacrylate) (PLMA), the structures of which are shown in Figure 1.

Experimental Section

Materials and Methods. Initial experiments showed that on contact with water thin films of the blends coated onto a silver substrate (required for the SPR experiments) were unstable and ruptured, probably due to the combination of a slight swelling of MPC-*co*-LMA and the weak forces holding the very hydrophobic PLMA to the hydrophilic silver. To help anchor the PLMA to the silver, hydrophobic methyl-terminated self-assembled monolayers (SAM's) were formed.

Preparation of Self-Assembled Monolayers (SAM's). The silver surface of the SPR sensors was initially cleaned by passing over a hydrogen flame to remove any adsorbed contaminants which may have hindered the formation of the SAM's. The slides were then incubated in a 1 mM solution of 1-dodecanethiol (Aldrich, Poole, Dorset, U.K.) in ethanol for 17 h. The slides were then rinsed in fresh ethanol and dried under a stream of nitrogen gas. All glassware used was cleaned with chromic acid prior to use.

Preparation of Polymer Films. PLMA was purchased from Aldrich (Poole, Dorset, U.K.) as a 25% (w/v) solution in toluene. The toluene was removed by heating to 60 °C for approximately 16 h. The preparation of the thin film consisting of only PLMA was performed at room temperature by spin-casting 130 μL of a 0.5% (w/v) polymer solution in chloroform onto a derivatized silver surface at approximately 2000 rpm. The MPC-*co*-LMA sample was provided by Biocompatibles PLC, Farnham, U.K. Thin-film preparation was performed as for the PLMA. To prepare the blended films of PLMA and MPC-*co*-LMA, the appropriate amounts of the polymers were dissolved together in chloroform and spun-cast as before.

Contact Angle Analysis. A drop of ultrapure water (5 μL) was placed on the surface of the sample being analyzed, and the angle formed at the solid−liquid interface was measured on each side. The mean value of 10 readings (both sides of five separate drops) was calculated for each sample.

AFM Analysis. AFM was carried out using a Multimode Nanoscope IIIa (Digital Instruments, Santa Barbara, CA). Tapping mode was employed in air using a tip fabricated from silicon (125 μm in length with ca. 300 kHz resonant frequency) and in liquid using a silicon nitride tip (V-shaped with force constant approximately 0.06 N m^{-1}). Topography and phase-detection images were obtained simultaneously as described previously.[17] Single-point amplitude−phase−distance ($a-p,d$) measurements were recorded for MPC-*co*-LMA, PLMA, and one of the polymer blends. The $a-p,d$ curves have been shown to be useful in defining imaging parameters and in helping to understand TMAFM images[25] and to identify components in heterogeneous samples.[25−27] Here, single-point $a-p,d$ measurements were used to "fingerprint" the components of the polymer blend by illustrating their different tip−sample interactions.

SPR Analysis. The SPR experiments were carried out using an instrument employing the Kretchmann configuration and a monochromatic laser source of 780 nm (Ortho Clinical Diagnostics, Buckinghamshire, U.K.). The instrument has been described in detail previously.[28] The SPR sensors consisted of glass slides with thin films of silver (approximately 50 nm thick) coated on one side. The polymers under investigation were cast onto the silver-coated side of the slides, previously derivatized with 1-dodecanethiol, which were then index-matched to the hemicylindrical prism of the SPR instrument by the application of immersion oil (BDH, Poole, Dorset, U.K.). Sodium phosphate buffer, pH 7.4, was flowed over the polymer surface at a rate of 0.24 mL/min. The temperature of the SPR sensor was allowed to stabilize at approximately 34 °C before a solution of fibrinogen (Sigma, Poole, Dorset, U.K.) in phosphate buffer (0.05 mg/mL) was introduced via the flow cell. Interaction of the protein with the polymer surfaces was detected by measuring the angle at which minimum reflectivity of the SPR laser on the sensor slide occurred, as recorded by a photodiode array.

Results

Formation of Methyl-Terminated SAM's. To ensure that the 1-dodecanethiol had reacted with the silver to produce a SAM, the hydrophobicity of the surface was monitored by recording the contact angle formed by a drop of water with the sample. Measurements were taken before and after cleaning in a hydrogen flame and after derivatization with the thiol solution. Before cleaning, the contact angle recorded ranged from 55° to 65°, which indicates that there is layer of hydrocarbon contaminant on the surface. After passing the silver through the hydrogen flame the minimum angle measured was 7°; however, within seconds this increased gradually as the surface became contaminated. After reaction of the silver with thiol solution the contact angle increased to 95 ± 0.5°, which is in good agreement with literature values,[29] suggesting that the reaction proceeded as expected.

AFM Analysis. The morphology of the single polymer systems, PLMA and MPC-*co*-LMA, characterized using TMAFM show the homogeneous nature of the polymer films when cast onto the silver slide. Figure 2, 2 μm × 2 μm topography (a) and phase (b) images of MPC-*co*-LMA, illustrates that there is no phase contrast present

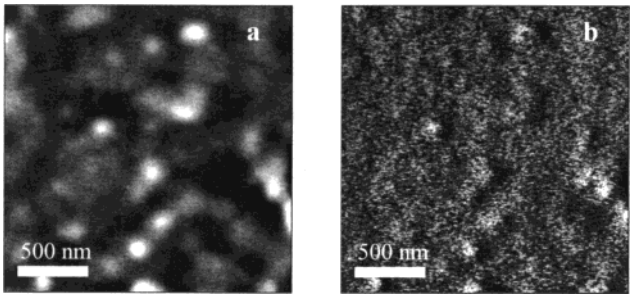

Figure 2. Height (a) and phase (b) images of MPC-*co*-LMA 2 μm × 2 μm area. Height range is 20 nm, and phase shift is 20°. The phase image shows no contrast apart from that which is topography induced, suggesting a uniform, homogeneous surface.

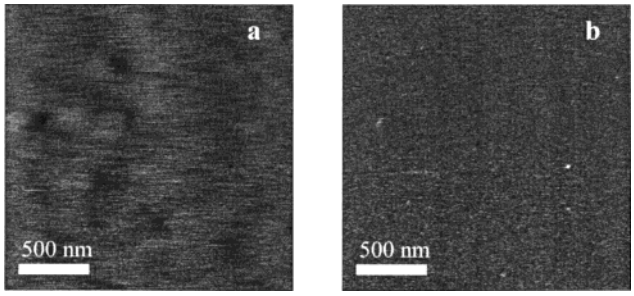

Figure 3. Height (a) and phase (b) images of PLMA 2 μm × 2 μm area. Height range is 5 nm, and phase shift is 5°. The phase image shows no contrast, suggesting a uniform, homogeneous surface.

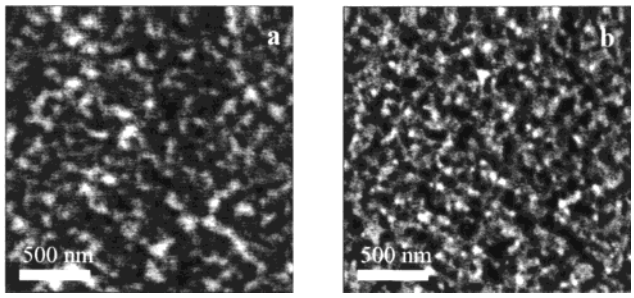

Figure 4. Height (a) and phase (b) images of a 2.88:1 PLMA:(MPC-*co*-LMA) blend, 2 μm × 2 μm area. Height range is 8 nm, and phase shift is 20°. Both topography and phase show a well-defined two-component system, with negligible contribution to the image from the silver substrate.

that can be identified as being caused by the polymer. The contrast seen in the phase image can be attributed to the contours of the underlying silver substrate. The equivalent images of PLMA, shown in Figure 3, again show no phase contrast caused by the polymer, and there are few features in the topography image suggesting a slightly thicker film than that cast for MPC-*co*-LMA. In addition to acting as a control for the imaging of the polymer blends, this confirmed that the technique used to coat the slides was efficient in providing a uniform coverage of the surface, free from holes or other defects which could have a detrimental effect on the SPR results. Figure 4 shows 2 μm × 2 μm images of the 2.88:1 (w/w) PLMA:(MPC-*co*-LMA) blend. Both the topography (a) and phase (b) images show a well-defined two-component system, with negligible contribution to the image from the silver substrate. The surface of the polymer can be seen to be dominated by one of the two polymers in the blend, with the other forming irregularly shaped nanometer-sized domains. With a composition consisting of 2.88:1 PLMA:(MPC-

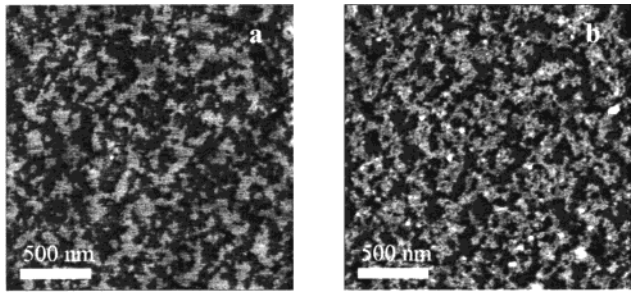

Figure 5. Height (a) and phase (b) images of a 4.54:1 PLMA:(MPC-*co*-LMA) blend, 2 μm × 2 μm area, with both components clearly visible. Height range is 5 nm, and phase shift is 20°.

co-LMA) it could be expected that the dominant region in the phase image, i.e., the light contrasted region, would be the PLMA component. By varying the composition of the blend and creating a range of compositions, this hypothesis was tested. Figure 5 shows 2 μm × 2 μm images of a blend having a ratio of PLMA:(MPC-*co*-LMA) of 4.54:1. Figure 5a shows the topographical image of the polymer surface. Here the phase segregation of the blend is more visible than in the previous sample due to reduced influence from the silver—a result of either a smoother substrate or a slightly thicker polymer film. The phase data in Figure 5b show this more clearly, and it can be seen that the amount of surface area covered by dark phase-contrast regions has increased, suggesting that the polymer responsible for this component of the image is actually PLMA. To confirm the identity of the phase-segregated regions found at the surface of the polymer blends, $a-p,d$ curves were recorded for pure PLMA, pure MPC-*co*-LMA, and the light and dark phase-contrast regions of the blends. Figure 6 shows the $a-p,d$ curves for PLMA and MPC-*co*-LMA. This indicates the difference in tip−sample interactions between the two polymers. Initially, as the tip approaches the surface, the amplitude and phase lag remain constant. As the tip makes contact, attractive forces dominate the tip−sample interactions and the amplitude decreases, accompanied by an increase in phase lag. As the tip continues to approach, eventually the repulsive forces between the tip and sample become greater than the attractive forces. This point can be seen clearly in Figure 6b, visible on the curve as a sudden increase in the amplitude and decrease in phase lag. Figure 6a illustrates that the jump from the attractive to repulsive region of the curve is less apparent in PLMA and appears as a smooth change in the gradient of the amplitude−distance curve and as a gradual decrease in phase lag. We believe this difference in behavior between the two samples and the tip can be explained by their different physical properties, as best illustrated by considering energy dissipation of the AFM cantilever during $a-p,d$ measurements. Energy dissipation can be determined from the $a-p,d$ curves and provide complementary information which aids their interpretation.[30] Figure 7 contains the amplitude−distance data as well as the energy dissipation data for both PLMA and MPC-*co*-LMA. Initially as the tip approaches both materials, the energy dissipation is zero. As the tip is brought to the PLMA rapid energy dissipation occurs, eventually becoming constant at an average energy dissipation of approximately 0.8 pW. For MPC-*co*-LMA energy dissipation initially occurs at a slower rate, becoming constant more rapidly at a lower energy dissipation of 0.05 pW. These data strongly suggest that the interaction between the AFM probe and

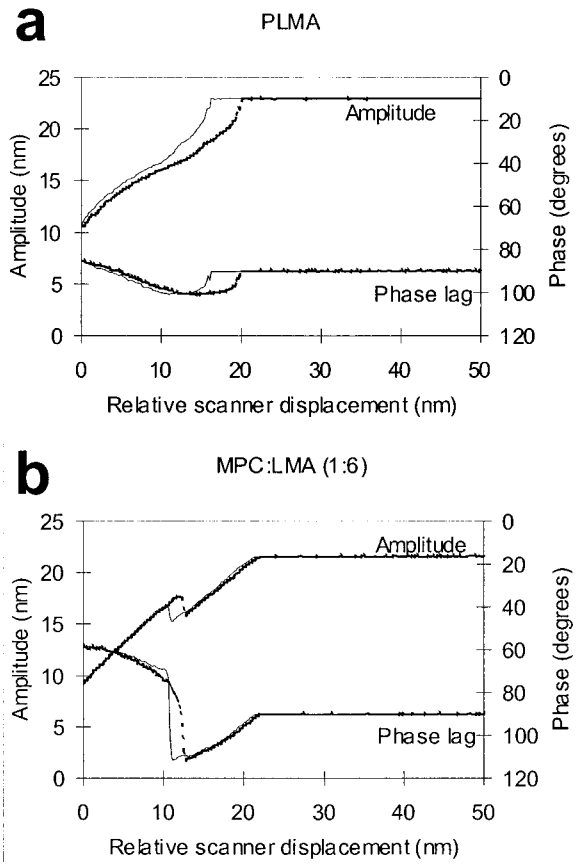

Figure 6. The *a*−*p*,*d* curves for PLMA (a) and MPC-*co*-LMA (b) showing the difference in tip−sample interactions of the two polymers. The thinner line indicates tip−sample approach data and the thicker retract data.

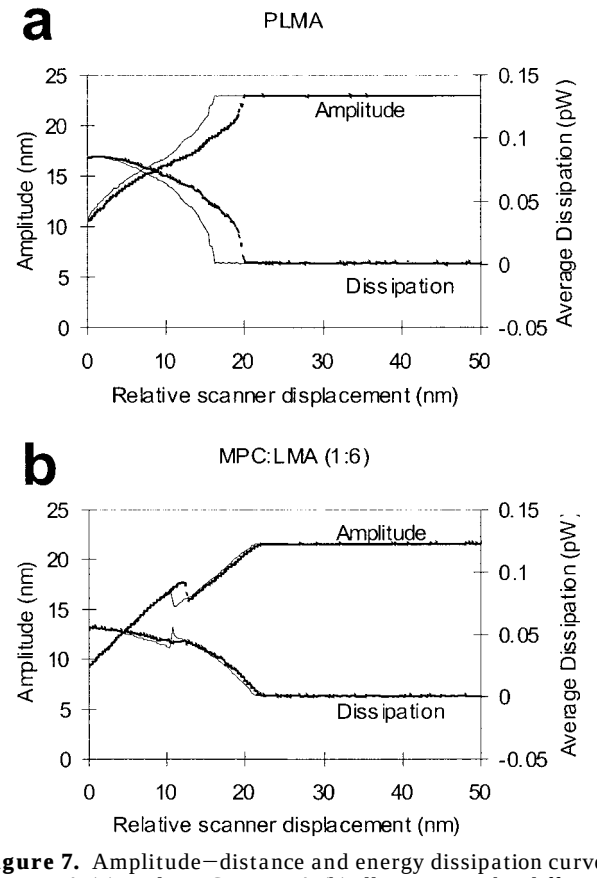

Figure 7. Amplitude−distance and energy dissipation curves for PLMA (a) and MPC-*co*-LMA (b) illustrating the different way in which the two materials absorb energy from the AFM cantilever upon contact. The thinner line indicates tip−sample approach data and the thicker retract data.

the MPC-*co*-LMA is a conservative process indicative of a largely elastic response from the MPC-*co*-LMA. Conversely, the PLMA displays nonconservative type behavior typical of a plastic type interaction. This is consistent with the macroscopic properties of the two materials: PLMA is a very sticky material which exists at room temperature as an extremely viscous liquid which displays plastic type behavior; MPC-*co*-LMA, although consisting of a large amount of lauryl methacrylate, contains the zwitterionic PC headgroup which adds a degree of crystallinity and hence elasticity to the material. Another difference in the *a*−*p*,*d* curves of PLMA and MPC-*co*-LMA which can be accounted for by their different physical properties is the hysteresis that occurs between the extend and retract data. As already stated, PLMA has an adhesive surface to which the AFM probe will stick inducing hysteresis. Although visible in the curves for MPC-*co*-LMA, hysteresis exists to a lesser degree due to the less adhesive surface. Hence, the phase contrast observed in the AFM imaging in air is most probably due to the differing nature of interaction of the PLMA and MPC-*co*-LMA. This is in contrast to the possible inducement of phase contrast by the formation of a capillary between the oscillating AFM probe and surface,[26] since in such a case the more hydrophilic MPC-*co*-LMA would be expected to have the higher surface water coverage and therefore the greater energy dissipation and darker phase contrast compared to the PLMA. However, the reverse contrast is observed.

Figure 8 contains the data recorded for the light and dark regions of a PLMA:(MPC-*co*-LMA) blend. Figure 8a shows the curve for the dark region of phase contrast; the amplitude−distance and phase−distance traces are comparable to those of the PLMA alone. Figure 8b shows data obtained from the light region of the blend and is comparable to the MPC-*co*-LMA alone. To compare the surface coverage of PLMA found by TMAFM with that calculated theoretically by ratioing of the masses of each component in the blend, bearing analysis was carried out on the phase images. The percentage surface coverage of each of the components in the blends was calculated using the Nanoscopes analysis software. Bearing analysis reveals how much of a surface lies above or below a given height (topography) or a given phase shift (phase) by counting the occurrence of pixels at various *Z* heights. Figure 9 highlights the change in surface coverage of the two components as the composition is changed. In the 4.54:1 PLMA:(MPC-*co*-LMA) the degree of surface coverage by the PLMA and MPC-*co*-LMA appears to approaching equality, with 57% of the surface being covered by the light-phase contrast region (calculated by counting the number of pixels above and below a threshold value in the phase image). In all blends analyzed, the amount of MPC-*co*-LMA found at the surface was significantly greater than could be expected if the surface composition was indicative of the bulk, suggesting that the surface free energy of the MPC-*co*-LMA is lower in air than that of the PLMA. A possible reason for this is the presence of the extremely hydrophilic PC headgroup. Previous work has shown that the extreme surface region of the copolymer is dominated by the LMA component[31] when in a nonaqueous environment, with the PC being buried in the bulk of the material. However, it is unlikely that there

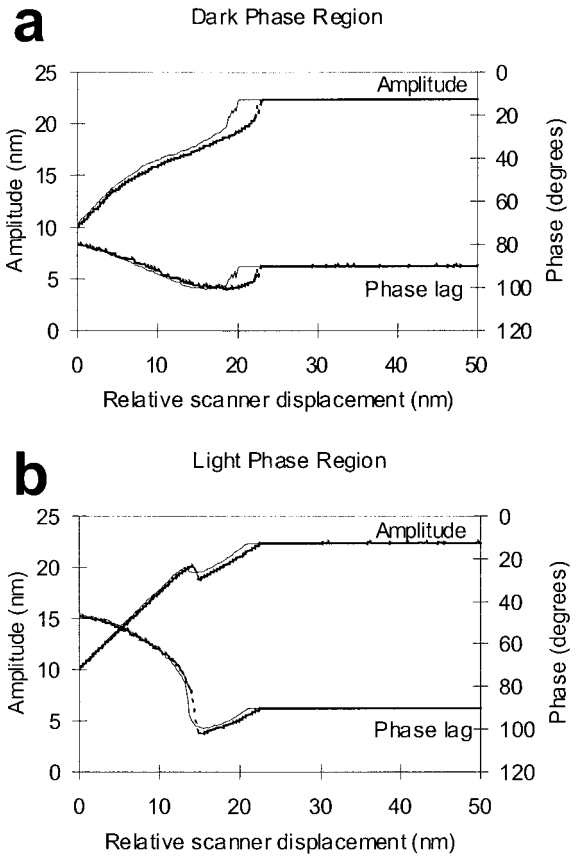

Figure 8. The $a-p,d$ curves for the dark (a) and light (b) regions of phase contrast in one of the blends. The difference in the traces can be used to identify which component of the blend is PLMA and which is MPC-*co*-LMA. The thinner line indicates tip−sample approach data and the thicker retract data.

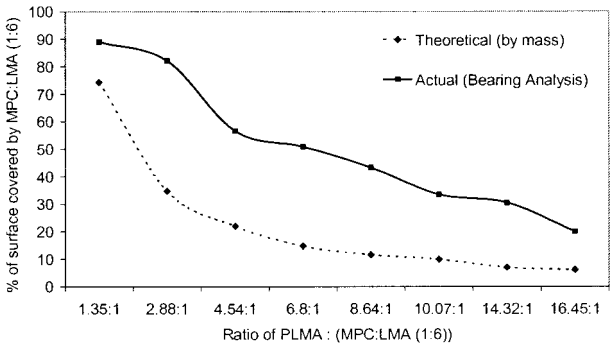

Figure 9. Comparison of the surface coverage of MPC-*co*-LMA calculated using Bearing Analysis to the expected coverage calculated from the actual composition of the blends.

is a total absence of PC at the surface owing to the random nature of the arrangement of the polymer chains when cast onto the substrate. So although the surface is hydrophobic, being mainly composed of the LMA moiety, it is possible that the PC that is present will influence the surface composition, causing the copolymer to be preferentially exposed due to the water vapor content of the atmosphere.

In addition to imaging the spun-cast blends, AFM was also used to visualize the materials in an aqueous environment to give an indication of how they would behave in the body. Figure 10 shows the 2.88:1 PLMA:(MPC-*co*-LMA) blend when submerged in ultrapure water. The nanometer-sized domains previously seen in Figure 4 appear to have disappeared, leaving a smooth

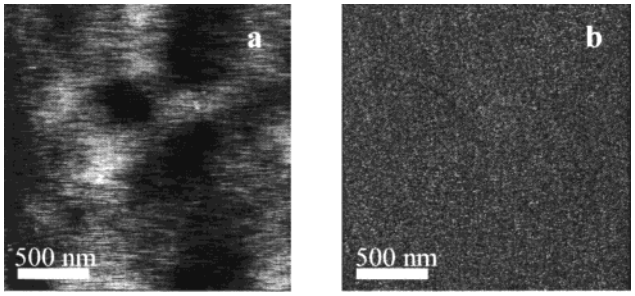

Figure 10. The 2 μm × 2 μm height (a) and phase (b) images of the 2.88:1 PLMA:(MPC-*co*-LMA) when submerged in water. The phase-segregated system is no longer visible in either the topography or phase images. Height range is 5 nm, and phase shift is 5°.

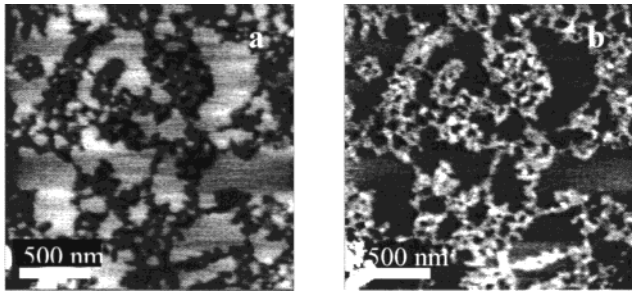

Figure 11. Height (a) and phase (b) images of the 6.81:1 PLMA:(MPC-*co*-LMA) after being wetted and then allowed to dry, confirming the stability of the coating in water. The two-component system is once again visible, but the distribution of the domains has changed as a result of the drying process. Height range is 20 nm, and phase shift is 10°.

surface with little topographical inhomogeneity, although there are areas of different heights visible. This could be due to the two blend components but could also be a result of the contours of the underlying silver substrate. The 6.8:1 PLMA:(MPC-*co*-LMA) blend was imaged under the same conditions, and again the two-phase system had been replaced by a homogeneous surface, this time with no evidence of the two components being visible, suggesting that the topography change seen before was due to the substrate. The lack of phase contrast in aqueous environments suggests a homogeneous surfaces has formed through rearrangement of the polymer components, possibly through a preferential expression of the hydrophilic PC groups at the surface. This hypothesis is consistent with the observation that in nonaqueous environments the hydrophobic LMA component becomes preferentially expressed at the surface.[31] To ensure that the films had remained stable throughout the liquid experiments, and would therefore maintain their integrity during the SPR analysis, the blends were imaged after being wetted and allowed to dry. Figure 11 shows the 6.8:1 PLMA:(MPC-*co*-LMA) blend after drying, and again phase segregation is clearly visible. However, the distribution patterns of the domains are different to those before the film came into contact with water. The change in appearance is likely to be caused by the swelling and surface rearrangement of the MPC-*co*-LMA component of the blend.

SPR Analysis. Figure 12 shows the SPR traces for the plasma-protein fibrinogen and the carrier-protein human serum albumin (HSA) being passed over PLMA (a) and MPC-*co*-LMA (b). In SPR, protein adsorption is accompanied by an increase in the angle of minimum light reflection (termed θ_{SPR}). Passing fibrinogen and

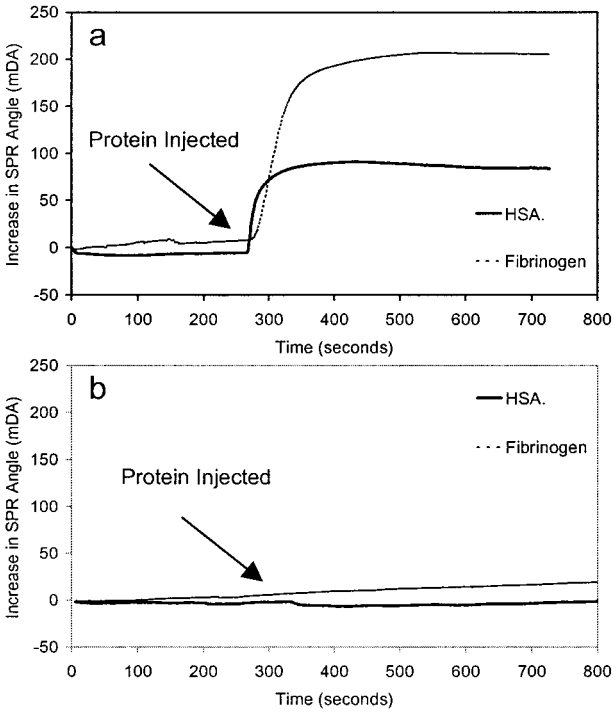

Figure 12. SPR trace showing the adsorption profiles of HSA and fibrinogen to PLMA (a) and MPC-*co*-LMA (b). It is clear that neither fibrinogen nor HSA adheres to the MPC-*co*-LMA but sticks to the PLMA.

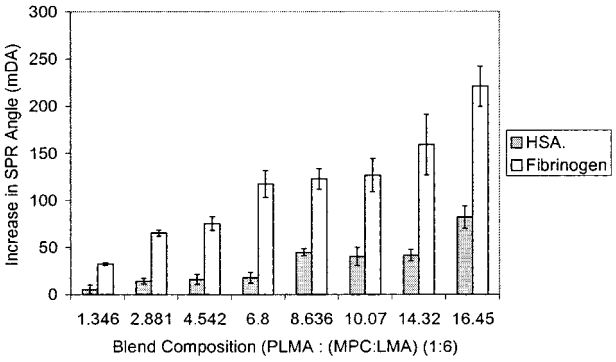

Figure 13. SPR results for the range of blends studied. It can be seen that there is a linear relationship between the amount of MPC-*co*-LMA contained in the blend and the amount of protein adsorbing to the surface. The composition of 16.45:1 PLMA:MPC-*co*-LMA shows an increase in θ_{SPR} equivalent to pure PLMA.

HSA over PLMA caused increases in θ_{SPR} of 206.9 ± 6.3 and 87.4 ± 3.0 mDA, respectively, while with MPC-*co*-LMA no increase was detected for either of the proteins. However, a small negative shift can be seen as the HSA passes over the surface. A possible explanation for this could be that although the protein does not adhere irreversibly to the material, there is an interaction that causes a slight change in the surface of the polymer. Figure 13 shows the SPR results for a range of blends of the PLMA and MPC-*co*-LMA. It can be seen that for the blend composition 1.35:1 PLMA:MPC-*co*-LMA there is little detectable protein adsorption to the polymer surface, with increases in θ_{SPR} of 5.25 ± 4.73 mDA for HSA and 32.34 ± 1.44 mDA for fibrinogen. As more PLMA is added to the blend, further adsorption occurs with the blend containing the ratio 16.45:1 PLMA:(MPC-*co*-LMA) showing increases in θ_{SPR} of 220 ± 21.1 mDA for fibrinogen and 88.89 ± 9.48 mDA for HSA in θ_{SPR} which are extremely close to those observed for pure PLMA. This suggests that this blend composition produces a surface with protein-resistant properties indistinguishable from PLMA.

Discussion

PLMA is a very hydrophobic polymer due to the $C_{12}H_{25}$ side chain and the long hydrocarbon backbone. In contrast, MPC-*co*-LMA is ampiphilic and contains the PC headgroup which has been shown to have a strong affinity for water[32] as a result of its zwitterionic structure. It has been hypothesized that the hydrophilicity of a materials surface has a major influence on the amount of protein that will adsorb,[33] and hence this could explain the behavior of these two polymers.

The observed deterioration in the protein-resistant nature of the coatings as the quantity of MPC-*co*-LMA in the material decreases is expected. However, the fact that a substantial amount of PLMA can be added before protein begins to adsorb to the polymer is not. The explanation as to why this occurs can be found from examination of the AFM images of the blends. In the 1.35:1 LMA:MPC-*co*-LMA the surface of the blend is dominated by the MPC-*co*-LMA moiety which covers over 85% of the surface area of the film. As MPC-*co*-LMA has been shown to prevent fibrinogen and albumin adsorption, it is clear that by being preferentially expressed at the surface, and so dominating the overall properties in this region, it is able to influence the level of protein resistance of the material. Indeed, even the 6.8:1 PLMA:(MPC-*co*-LMA) blend, which has an approximately equal surface coverage of the two components, shows a reduction in fibrinogen adsorption of nearly 50% compared to pure PLMA. An explanation as to why the copolymer is expressed preferentially at the surface over the homopolymer could be due to micellization. Shull et al.[34] have showed that in polymer blends of polystyrene and a block copolymer of deuterated polystyrene and poly(2-vinylpyridine) that the copolymer preferentially segregates to the surface of the material. This phenomenon has been explained as a manifestation of attractive interactions between polymer brushes and a free surface. Although the MPC-*co*-LMA polymers studied here are random in nature, it is still feasible that these forces exist which would result in the copolymer-enriched surface observed. A possible reason for the enhanced biocompatibility is related to the size of the domains formed by the two constituents of the blends. Many polymer blends exhibit surface phase segregation of the components, with the resultant domains having micrometer-sized dimensions. The AFM images obtained from the PLMA-(MPC-*co*-LMA) blends show much smaller regions that are irregular in shape and nanometers in dimensions. Although fibrinogen and human serum albumin are small relative to these domains, it seems likely that a surface such as this makes it more difficult for the protein molecules to find a suitable binding site. As the PLMA becomes the predominant moiety, a much greater percentage of the surface is rendered nonbiocompatible, and so the ease with which binding sites can be found by the fibrinogen molecules is increased. Another possibility for the enhanced protein resistance could be related to the extreme hydrophilicity of the PC headgroup contained within the MPC-*co*-LMA. When hydrophilic polymers are submerged in water, they can hydrate, swell, and undergo a surface rearrangement. As a result of the

MPC-*co*-LMA copolymer having both extremely hydrophilic and hydrophobic components, this rearrangement causes a large change in the surface region.

Conclusions

TMAFM phase images of the PLMA:MPC-*co*-LMA mixtures showed that the two components are immiscible and when cast from a solution exhibit surface segregation when produced as thin films. The MPC-*co*-LMA moiety is preferentially expressed at the surface of the blends, giving protein-resistant properties. The nanometer-sized domains formed by the two polymers in the blends appear to aid in preventing fibrinogen and HSA adsorbing to the surface of the materials, with the amount of protein adhering being lower than could be expected from the percentage of PLMA exposed. This illustrates the high level of biocompatibility produced by incorporation of only a small amount of the PC headgroup into a material. By investigating how the MPC-*co*-LMA interacts with other polymers which are already used in biomaterial applications when blended together, it may be possible to tailor materials that retain the useful features of both components. This could ultimately lead to the development and production of new materials with great potential for a wide range of biomedical applications.

Acknowledgment. S.C. thanks the EPSRC and Biocompatibles Ltd. for providing funding through a CASE award.

References and Notes

(1) *Biomaterials Science*; Ratner, B. D., Hoffman, A. S., Schoen, F. J., Lemons, J. E., Eds.; Academic Press: New York, 1996.
(2) Van Oeveren, W.; Kazatchine, M. D.; Descamps-Latscha, B.; Maillet, F.; Fischer, E.; Carpentier, A. *J. Thorac. Cardiovasc. Surg.* **1985**, *89*, 888.
(3) Hayward, J. A.; Chapman, D. *Biomaterials* **1984**, *5*, 135.
(4) Campbell, E. J.; O'Byrne, V.; Stratford, P. W.; Quirk, I.; Vick, T.; Wiles, M. C.; Yianni, Y. P. *Am. Soc. Artifical Internal Organs J.* **1994**, *40*, M853.
(5) Murphy, E. F.; Ju, J. R.; Brewer, J.; Russell, J.; Penfold, J. *Langmuir* **1999**, *15*, 1313.
(6) Ishihara, K.; Iwasaki, Y.; Nakabayashi, N. *Mater. Sci. Eng.* **1998**, *C6*, 253.
(7) von Segesser, L. K.; Tonz, B.; Leskosek, M.; Turina, M. *Am. Soc. Artificial Internal Organs* **1994**, *17*, 294.
(8) Ueda, T.; Oshida, H.; Kurita, K.; Ishihara, K.; Nakabayashi, N. *Polym. J.* **1992**, *24*, 1259.
(9) Ruiz, L.; Hilborn, J. G.; Léonard, D.; Mathieu, H. J. *Biomaterials* **1998**, *19*, 987.
(10) Zhang, S. F.; Rolfe, P.; Wright, G.; Lian, W.; Milling, A. J.; Tanaka, S.; Ishihara, K. *Biomaterials* **1998**, *19*, 691.
(11) van der Heiden, A. P.; Willems, G. M.; Lindhout, T.; Pijpers, A. P.; Koole, L. H. *J. Biomed. Mater. Res.* **1998**, *40*, 195.
(12) Oishi, T.; Uchiyama, H.; Onimura, K.; Tsutsumi, H. *Polym. J.* **1998**, *30*, 17.
(13) Korematsu, A.; Murakami, T.; Sakuri, I.; Kodama, M.; Nakaya, T. *J. Mater. Chem.* **1999**, *9*, 647.
(14) Viville, P.; Thoelen, O.; Beauvois, S.; Lazzaroni, R.; Lambin, G.; Bredas, J. L.; Kolev, K.; Laude, L. *Appl. Surf. Sci.* **1995**, *86*, 411.
(15) Muller-Buschbaum, P.; O'Neill, S. A.; Affrossman, S.; Stamm, M. *Macromolecules* **1998**, *31*, 5003.
(16) Slep, D.; Asselta, J.; Rafailovich, M. H.; Sokolov, J.; Winesett, D. A.; Smith, A. P.; Ade, H.; Strzhemechny, Y.; Scwarz, S. A.; Sauer, B. B. *Langmuir* **1998**, *14*, 4860.
(17) Chen, X.; McGurk, S. L.; Davies, M. C.; Roberts, C. J.; Shakesheff, K. M.; Tendler, S. J. B.; Williams, P. M.; Davies, J.; Dawkes, A. C.; Domb, A. *Macromolecules* **1998**, *31*, 2278.
(18) Takahara, A.; Jiang, X.; Satomi, N.; Tanaka, K.; Kajiyama, T. *Key Eng. Mater.* **1998**, *137*, 79.
(19) Shakesheff, K. M.; Chen, X.; Davies, M. C.; Domb, A.; Roberts, C. J.; Tendler, S. J. B.; Williams, P. M. *Langmuir* **1995**, *11*, 3921.
(20) van Delden, C. J.; Lens, J. P.; Kooyman, R. P. H.; Engbers, G. H. M.; Feijen, J. *Biomaterials* **1997**, *18*, 845.
(21) Green, R. J.; Davies, J.; Davies, M. C.; Roberts, C. J.; Tendler, S. J. B *Biomaterials* **1997**, *18*, 405.
(22) Ishihara, K.; Tanaka, S.; Furukawa, N.; Kurita, K.; Nakabayashi, N. *J. Biomed. Mater. Res.* **1996**, *32*, 391.
(23) Ishihara, K.; Tanaka, S.; Furukawa, N.; Kurita, K.; Nakabayashi, N. *J. Biomed. Mater. Res.* **1996**, *32*, 401.
(24) Yoneyama, T.; Ishihara, K.; Nakabayashi, N.; Ito, M.; Mishima, Y. *J. Biomed. Mater. Res.* **1998**, *43*, 15.
(25) Chen, X.; Davies, M. C.; Roberts, C. J.; Tendler. S. J. B.; Williams, P. M.; Davies, J.; Dawkes, A. C.; Edwards, J. C. *Ultramicroscopy* **1998** *75*, 171.
(26) Danesh, A.; Chen, X.; Davies, M. C.; Roberts, C. J.; Sanders, G. W. H.; Tendler, S. J. B.; Williams, P. M.; Wilkins, M. J. *Langmuir* **2000**, *16*, 866.
(27) Baker, A. A.; Miles, M. J.; Helbert, W. *Carbohydr. Res.* **2001**, *330*, 249.
(28) Davies, J. *Nanobiology* **1994**, *3*, 15.
(29) Batin, C. D.; Troughton, E. B.; Tao, Y.-T.; Evall, J.; Whitesides, G. M.; Nuzzo, R. G. *J. Am. Chem. Soc.* **1989**, *111*, 321.
(30) Cleveland, J. P.; Anczykowski, B.; Schmid, A. E.; Elings, V. B. *Appl. Phys. Lett.* **1998**, *72*, 2613.
(31) Clarke, S.; Davies, M. C.; Roberts, C. J.; Tendler; S. J. B.; Williams, P. M.; Lewis, A. L.; Russell, J.; O'Byrne, V. *Langmuir* **2000**, *16*, 5116.
(32) Salsbury, N. J.; Darke, A.; Chapman, D. *Chem. Phys. Lipids* **1972**, *8*, 142.
(33) Rabinow, B. E.; Ding, Y. S.; Qin, C.; McHalsky, M. L.; Schnieder, J. H.; Ashline, K. A.; Shelbourn, T. L.; Albrecht, R. M. *J. Biomat. Sci. Polym. Ed.* **1994**, *6*, 91.
(34) Shull, K. R.; Winey, K. I.; Thomas, E. L.; Kramer, E. J. *Macromolecules* **1991**, *24*, 2748.

MA0016681